communications earth & environment

Article

A Nature Portfolio journal

https://doi.org/10.1038/s43247-025-02468-x

Copper isotope evidence for recycled crustal sulfides in deep mantle plume source

Junhua Yao[1], Wei Yuan[2] ✉, Zhengrong Wang[3,4], Frédéric Moynier[5], Wei-Guang Zhu[6], Ya-Dong Wu[7], Yuchen An[2] & Jiubin Chen[2] ✉

Earth's crustal materials are recycled into the mantle through subduction, but the depth and nature of recycled components remain debated. Here we report copper (Cu) isotope evidence for the involvement of recycled crustal materials in a deep-mantle plume source. Permian mantle plume-derived picrites and basalts from the Emeishan large igneous province (Southwest China), excluding three hydrothermally altered outliers, exhibit δ^{65}Cu values up to 0.65‰, obviously higher than typical mantle values (0.07 ± 0.10‰). The δ^{65}Cu values show no correlation with loss-on-ignition (LOI), Mg#, $\varepsilon_{Nd(t)}$, Cu/Th, Cu/Pd, or redox state, ruling out magma differentiation or post-magmatic alteration. Instead, the elevated δ^{65}Cu values most plausibly reflect recycled crustal sulfides with elevated δ^{65}Cu value in the mantle source. These findings provide robust evidence for the recycling of Cu-rich sulfides into the deep mantle (potentially the lower mantle), elucidating the ultra-deep geochemical cycling of copper and sulfur within Earth's interior.

Tracing recycled components in Earth's deep mantle is essential for developing a comprehensive understanding of mantle compositions and elemental cycles[1–3]. Mantle-derived volcanic rocks provide valuable insights into the nature of the deep mantle at various depths, ranging from the lithospheric mantle to the sub-arc mantle, mantle transition zone, and lower mantle[1,2,4–6]. Early studies mainly focused on radiogenic isotopes (including Sr-Nd-Pb-Hf-Os isotopes) and traditional stable isotopes (including C-O-S-H isotopes) in volcanic rocks, which have helped constrain the presence of recycled silicate components in Earth's mantle[1,4,7–9]. However, more recent studies have shifted attention to the stable isotope compositions of certain metals (such as Mg-Zn-Mo), offering the potential to trace different types of recycled components (including subducting sedimentary carbonates, crustal sulfides and organic materials) into the deep mantle[10–12].

Copper (Cu) is a key element in studying deep mantle processes due to its highly chalcophile (sulfur-loving) and redox-sensitive characteristics. The Cu isotope compositions of geological samples are strongly influenced by oxygen fugacity[13] and exhibit substantial variations in low-temperature supergene processes, compared with basalts and mantle rocks[14,15]. Some volcanic rocks, such as those from Mariana Arc and southern Okinawa Trough (with δ^{65}Cu values ranging from +0.26‰ to +0.67‰), and metasomatized mantle peridotites/pyroxenites from southeastern Arizona (with δ^{65}Cu values ranging from −0.29‰ to +3.88‰), exhibit higher or lower δ^{65}Cu values than the normal mantle value (δ^{65}Cu = 0.07 ± 0.10‰)[16]. These variations have been attributed to processes such as the addition of recycled crustal Cu-rich materials or metasomatism of oxidizing melts or fluids in the upper mantle[17,18]. However, the mechanisms behind copper isotope fractionation during magmatic processes remain a subject of debate. While these studies provide preliminary insights into the Cu cycle in the upper mantle, our understanding of Cu in deeper mantle reservoirs remains limited.

Oceanic hotspots (e.g., Hawaii, Iceland) and certain Large Igneous Provinces (LIPs) (e.g., Emeishan, Siberia) are believed to originate from deep-seated mantle plumes, which provide critical insights into the composition and dynamics of Earth's deep interior[4,8,19–22]. Compared with mid-ocean ridge basalts (MORBs) and oceanic island basalts (OIBs), continental intraplate basalts display a broader range of Cu isotope composition[23,24] (Fig. 1). Understanding these variations in Cu isotope composition is crucial to reveal the nature of Earth's deep copper reservoirs. In this study, we

[1]Key Laboratory of Ocean Observation and Forecasting, Center of Deep Sea Research Institute of Oceanology, Chinese Academy of Sciences, Qingdao, China. [2]Institute of Surface-Earth System Science, School of Earth System Science, Tianjin University, Tianjin, China. [3]Department of Earth and Atmospheric Sciences, The City College of New York, CUNY, New York, NY, USA. [4]Graduate Center, CUNY, New York, NY, USA. [5]Université Paris Cité, Institute de Physique du Globe de Paris, CNRS UMR7154, 1 rue Jussieu, Paris, France. [6]State Key Laboratory of Ore Deposit Geochemistry, Institute of Geochemistry, Chinese Academy of Sciences, Guiyang, China. [7]State Key Laboratory of Lithospheric Evolution, Institute of Geology and Geophysics, Chinese Academy of Sciences, Beijing, China. ✉e-mail: yuan_wei@tju.edu.cn; jbchen@tju.edu.cn

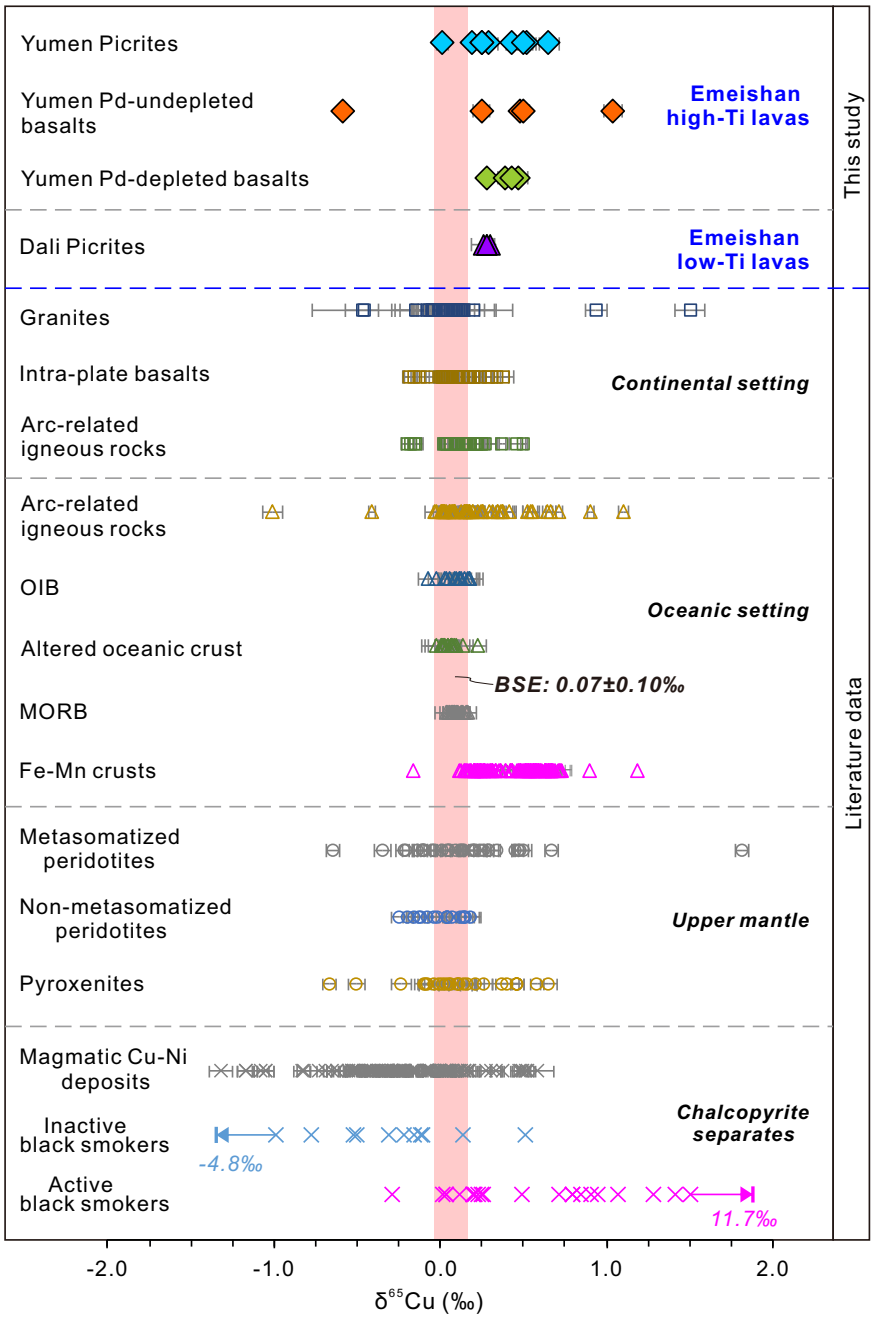

Fig. 1 | The whole-rock δ^{65}Cu values of the Emeishan lavas in comparison with peridotites, basalts, and other geological reservoirs reported in literatures. The Emeishan lavas (this study), bulk silicate earth (BSE)[16], other data (reference listed in Supplementary Note 2). Error bars are 2 standard deviation (SD).

present high-precision Cu isotope compositions for a series of samples from the Emeishan Large Igneous Province (ELIP) in southwest China. These samples include eighteen high-Ti picrites and basalts from the Yumen area and four low-Ti picrites from the Dali area (Fig. S1). The ELIP, interpreted as originating from the decompression melting of a mantle-plume head within the spinel stability field (<100 km depth)[25,26], comprises a wide range of basaltic rocks, minor picrites, and rare komatiites, forming a diverse picritic-basaltic magma series[26–28]. The low-Ti magmas of ELIP, characterized by a Ti/Y ratio of <500, show lower oxygen fugacity (fO_2: ~QFM + 0.3) than those of high-Ti series with Ti/Y > 500 (fO_2: ~QFM + 2)[29–31]. Further details on the geological setting, petrography, and previously published geochemical features for the collected samples are provided in Supplementary Note 1. Through analytical Cu isotope data, we assess the potential effects of magmatic processes and varying fO_2 levels on Cu isotope fractionation, estimate the Cu isotope composition of the mantle source in ELIP, and explore the implications for recycled components in Earth's deep interior (e.g., the lower mantle) and the deep cycling of Cu-rich sulfides.

Results and discussion

Whole-rock Cu isotope compositions

The Cu isotope compositions, along with previously published data on whole-rock elemental data (including major, trace, and platinum-group elements) and Sr-Nd isotope compositions of Emeishan volcanic rocks, are compiled in Supplementary Data 1. Detailed major and trace element compositions for the two studied low-Ti picrites from the Dali area are presented in Supplementary Note 2.

As illustrated in Fig. 1, the majority of Emeishan samples from the ELIP (including nine high-Ti picrites and nine high-Ti basalts from Yumen area, and four low-Ti picrites from Dali area) exhibit δ^{65}Cu values higher than MORB and OIB (δ^{65}Cu = −0.07‰ to +0.18‰)[23,24], and the Bulk Silicate Earth (BSE, 0.07 ± 0.10‰)[16]. Only two exceptions are observed: one picrite (YBYM1306) and one Palladium (Pd)-undepleted basalt (YBYM1603) from Yumen area. The Emeishan picrites show a relatively narrow range of δ^{65}Cu values. High-Ti picrites (from Yumen) have δ^{65}Cu values ranging between 0.01‰ and 0.65‰, while δ^{65}Cu values of low-Ti picrites (from

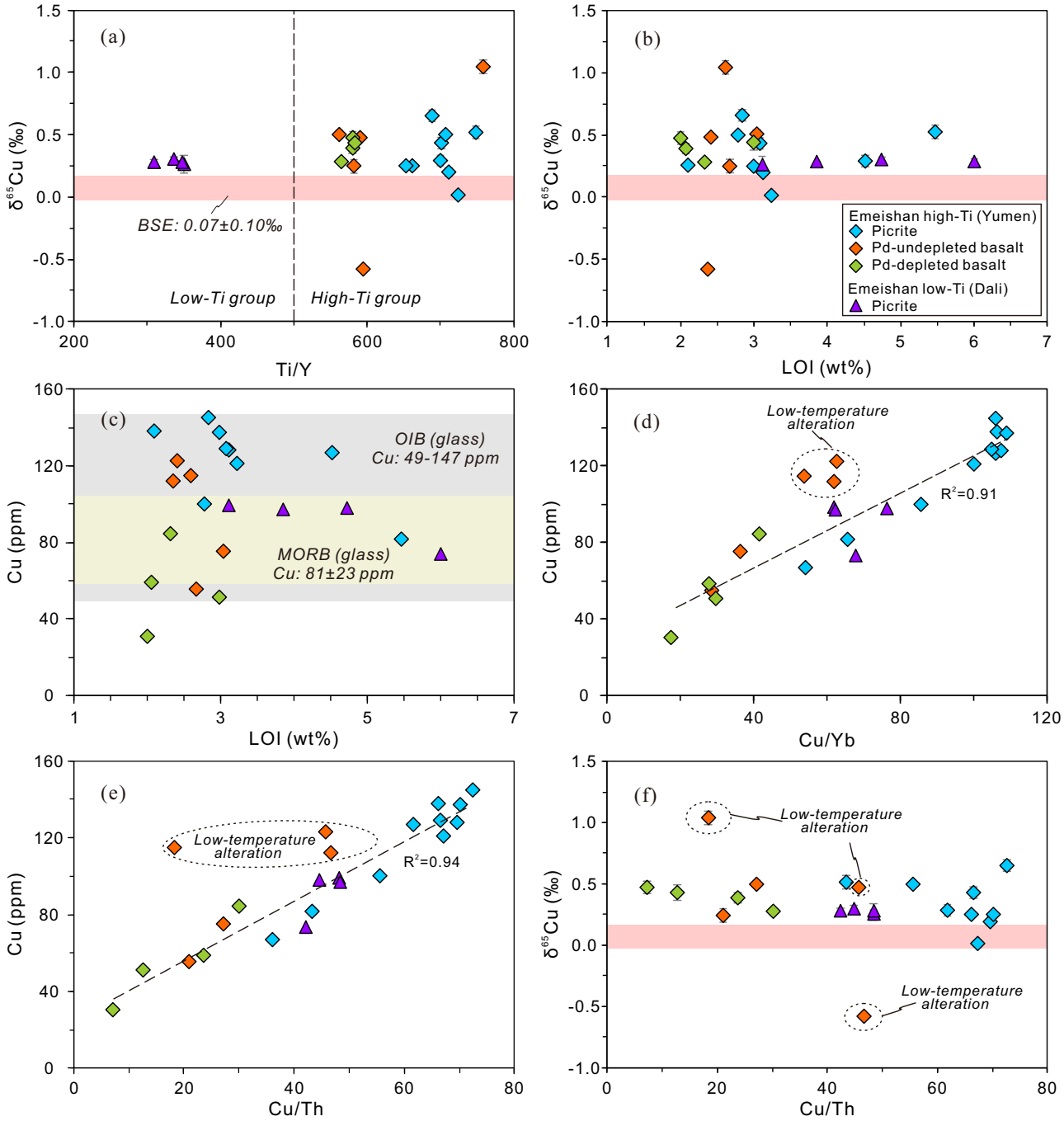

Fig. 2 | Relationships between whole-rock δ^{65}Cu isotope compositions, Cu abundances, and geochemical proxies indicative of Cu loss or enrichment in the Emeishan lavas. δ^{65}Cu versus Ti/Y (**a**), and loss on ignition (LOI) (**b**), and Cu versus LOI (**c**), Cu/Yb (**d**), Cu/Th (**e**), and δ^{65}Cu versus Cu/Th (**f**). **c** The gray and yellow bands represent the Cu content ranges of OIB and MORB glass samples, respectively. Data source: BSE[16], MORB and OIB[70]. Error bars are 2 SD.

Dali) cluster between 0.26‰ and 0.30‰ (Figs. 1 and 2a). In contrast, the Emeishan basalts exhibit highly variable Cu isotope compositions, with δ^{65}Cu values ranging from −0.58‰ to +1.04‰, which displays a range far exceeding that reported for other continental intraplate basalts (Fig. 1).

As a platinum-group element (PGE), palladium (Pd) exhibits extremely high partition coefficients (≈1.7×10^4) between immiscible sulfide melt and silicate melt[32], giving it a far stronger affinity for sulfide liquids than Ni, Cu and lithophile elements (e.g., Yb). This contrasting partitioning behavior makes elemental ratios such as Cu/Pd and Pd/Yb highly sensitive tracers of sulfide melt segregation, a process that can markedly influence δ^{65}Cu values. Following Li et al.[33], we apply a threshold of $10^5 \times (Pd/Yb) < 100$ to identify Pd depletion linked to magmatic sulfide melt saturation and segregation. Using this criterion, the Emeishan basalts are classified into two groups: Pd-depleted (samples affected by sulfide melt segregation) and Pd-undepleted (samples retaining primary magmatic signatures). Notably, Pd-undepleted basalts exhibit δ^{65}Cu values spanning from −0.58‰ to +1.04‰, over sixfold greater than the variability observed in MORB and OIB (δ^{65}Cu = −0.07‰ to +0.18 ‰)[23,24]. In contrast, Pd-depleted basalts show a more constrained δ^{65}Cu range of 0.28‰ to 0.47‰.

The influence of hydrothermal alteration

Low-temperature hydrothermal alteration can drive substantial Cu isotope fractionation, with altered rocks exhibiting δ^{65}Cu values ranging from −16.96‰ and +9.98‰[14,15], as stable isotope fractionation factor typically

increases with decreasing temperature[34–36]. Despite the high loss-on-ignition (LOI) values in most of our samples, a common indicator of post-magmatic alteration, four lines of evidence (detailed in the next section) indicate that low-temperature processes have not substantially affected their Cu isotope compositions. Exceptions include three Pd-undepleted basalts, two of which display extreme δ^{65}Cu values.

First, no clear correlation exists between δ^{65}Cu values and common indicators of chemical alteration, such as LOI and the chemical index of alteration (CIA: $Al_2O_3/(Na_2O + K_2O + Al_2O_3 + CaO) \times 100$, mol) (Fig. 2b and Fig. S2a). Second, previous studies[37,38] have shown that low-temperature alteration can result in remarkable loss of Cu in rocks (up to 90%), leading to Cu isotope fractionation. However, the whole-rock Cu contents of our samples (31 ppm to 145 ppm) overlap with those of fresh OIBs and show no covariation with LOI (Fig. 2c and Fig. S2b), suggesting minimal Cu mobilization. Given that Yb and Th are fluid-immobile under oxic conditions near Earth's surface and that Pd-undepleted basalts have not undergone sulfide segregation, variations in whole-rock Cu content along with Cu/Yb and Cu/Th ratios could be used to evaluate potential effects of low-temperature fluids or sulfide accumulation on whole-rock Cu. Most samples display a strong positive correlation between Cu and Cu/Yb or Cu/Th ($R^2 > 0.9$), while three Pd-undepleted basalts deviate from this trend (Fig. 2d–e), likely reflecting Cu variation caused by either of these processes. Third, the most extreme δ^{65}Cu values (−0.58‰ and 1.04‰) are observed in two of these three basalts, while the remaining samples have a relatively limited variation in δ^{65}Cu values (Fig. 2f). These two samples with extreme δ^{65}Cu values also exhibit extreme (lowest and highest) rubidium (Rb) contents, a moderately fluid-mobile element susceptible to fluid-related processes (Fig. S2c), further supporting the idea that these two extreme outliers result from low-temperature alteration. Lastly, due to their strong affinity for sulfides, both Cu and Pd exhibit similar behavior during basaltic magma differentiation. In a Cu versus Pd diagram (Fig. 3a), these three samples slightly deviate from the trend defined by other samples, displaying Pd contents slightly lower than other Pd-undepleted samples. This is inconsistent with the effect of the magma sulfide accumulation in the rock samples. Therefore, we infer that low-temperature alteration not only modified the Cu isotope compositions but also facilitated the redistribution of some fluid-mobile elements (e.g., Rb, Cu) in these three samples, while its influence on the remaining Emeishan samples was minimal. In order to better constrain the chemical behavior of Cu during magmatic evolution and the Cu isotope composition of the mantle source in ELIP, these three outlier samples will be excluded from subsequent discussions.

The influence of magmatic processes

Experimental studies demonstrate that in silicate melt, Cu^+ dominates under reducing conditions ($\Delta FMQ \leq +1.2$), whereas Cu^{2+} becomes prevalent at higher oxygen fugacity fO_2 ($\Delta FMQ \geq +1.2$)[39]. Theoretically, the fractional crystallization of early-stage Fe^{2+}-rich silicate minerals (e.g., olivine, clinopyroxene), without cotectic crystallization of Fe^{3+}-rich spinel, increases the Fe^{3+}/Fe^{2+} ratio in the residual silicate melt. This elevated ratio raises the oxygen fugacity (fO_2) of the magma, promoting the redox-driven reaction ($Cu^+ \rightarrow Cu^{2+}$)[40]. In sulfide-undersaturated melts, Cu behaves incompatibly, leading to its enrichment in evolved melts. Because the heavier isotope ^{65}Cu preferentially partitions into Cu^{2+} species[41], this redox process fractionates Cu isotopes, enriching the residual magma with heavier Cu isotope (^{65}Cu)[40]. Moreover, while co-precipitation of spinel with olivine may buffer fO_2 of magma, spinel preferentially uptakes the lighter isotope (^{63}Cu)[42], driving the residual melt toward heavier Cu isotope compositions. However, such isotopic enrichment of heavier Cu isotope is likely negligible unless substantial fractional crystallization of spinel and olivine occurs, as Cu isotope fractionation factors are inherently small at magmatic temperatures[23,43].

Geochemical data from the Emeishan picrites and basalts indicate that these rocks mainly underwent fractional crystallization of olivine and clinopyroxene, with a minor amount of spinel[44]. However, their whole-rock δ^{65}Cu values show no systematic correlation with indices of magmatic differentiation, such as Mg# (Fig. 3b) or Cr content (Fig. 3c). Moreover, no clear correlation is observed between V/Sc and δ^{65}Cu values (Fig. 3d), despite the wide range of V/Sc ratios (from 8 to 16), which likely reflects variations in oxidation state of magma. This lack of correlation suggests that early-stage fractional crystallizations of mafic minerals from basaltic magma result in limited Cu extraction, insufficient to induce appreciable Cu isotope fractionation. In addition, Cu isotope fractionation has not been documented during the fractional crystallization of sulfur-undersaturated magma[23,43]. These findings collectively indicate that magmatic fractional crystallization has a negligible impact on Cu isotope variability in the Emeishan samples.

Because the continental crust exhibits markedly elevated $^{87}Sr/^{86}Sr$ ratios, as well as lower ε_{Nd} and Nb/La ratios relative to the mantle, these geochemical parameters serve as robust indicators of crustal contamination. Sr–Nd isotope compositions suggest negligible crustal contamination in the Emeishan picrites and less than 10% contamination in the Emeishan basalts[44]. However, this minor level of crustal contamination is unlikely to affect the δ^{65}Cu values of Emeishan basalts. Typical upper continental crusts, as well as I-type and S-type granites, exhibit δ^{65}Cu values of 0.03 ± 0.15‰ and −0.03 ± 0.42‰, respectively[45], which overlap with the range of Cu isotope composition in MORBs. Lower crustal rocks tend to exhibit heterogeneous Cu isotope compositions that negatively correlate with Cu content[46]. Even using a lower crustal rock with the highest δ^{65}Cu value (2.5‰) as an end-member, a simple mixing calculation based on Cu-Nd isotopes shows that less than 10% lower crustal contamination would have an insignificant effect on Cu isotope composition in the magma. This would not account for the heavy Cu isotope compositions observed in our samples (Fig. 3e), as lower crustal rocks with high δ^{65}Cu values have very low Cu contents (as low as 20 ppm)[46]. Detailed compositions of the end-members in the binary mixing model are listed in Supplementary Data 2. This conclusion is further supported by the lack of correlations between δ^{65}Cu values and some other chemical indices such as Nb/La or $^{87}Sr/^{86}Sr$ ratios in these samples (Fig. S2d–e). Additionally, while the assimilation of crustal sulfur is known to trigger magmatic sulfide saturation and Pd depletion in the Emeishan basalts[44], the δ^{65}Cu values of Pd-depleted basalt samples align closely with those of the uncontaminated picrites (Fig. 3f). Thus, crustal contamination has a negligible effect on Cu isotope compositions in the Emeishan picrites-basalts.

Mantle-derived basaltic magma often experiences sulfide melt saturation and segregation of immiscible sulfide droplets or minerals during processes such as fractional crystallization, crustal contamination, mixing with hydrous fluids at depth, or rapid magma ascent[26,47,48]. During these events, Cu is preferentially partitioned into sulfide melts due to its high compatibility in sulfides[49]. If substantial Cu isotope fractionation occurs between sulfide melt and silicate melt, this segregation could substantially alter the δ^{65}Cu values of the residual silicate melt. However, previous studies showed that the Cu isotope fractionation factor (α) between sulfide melt and silicate melt is highly variable, displaying both negative to positive values. For example, results of lab experiments[16,50] and natural samples[40,43] have shown that sulfide melt can preferentially incorporate light Cu isotope ($\alpha < 1$), leading to higher δ^{65}Cu values in the remaining silicate melt. In contrast, a study of mantle pyroxenites from the Balmuccia massif indicates that segregated sulfide melt can, in some cases, prefer heavier Cu isotopes, with a fractionation factor $\alpha > 1$[51]. Moreover, studies on arc magmas and magmatic Ni–Cu sulfide deposits have shown very limited Cu isotope fractionation during sulfide segregation, with α value close to one[17,52,53].

Pd depletion in basalts serves as a reliable indicator of magmatic sulfide segregation due to the extremely high partition coefficient of Pd in sulfide melts. The δ^{65}Cu values of Yumen Pd-depleted basalts fall within the range of the Yumen picrites and Pd-undepleted basalts. Moreover, no correlations are observed between δ^{65}Cu values and Pd/Yb or Cu/Pd ratios in these samples (Figs. 3f and S2f). Although MORBs are generally believed to be saturated with sulfide melts[54], and some OIB samples show evidence of sulfide segregation[55], OIBs and MORBs typically exhibit δ^{65}Cu values consistent with ranges of the mantle and komatiites (between −0.07‰ and

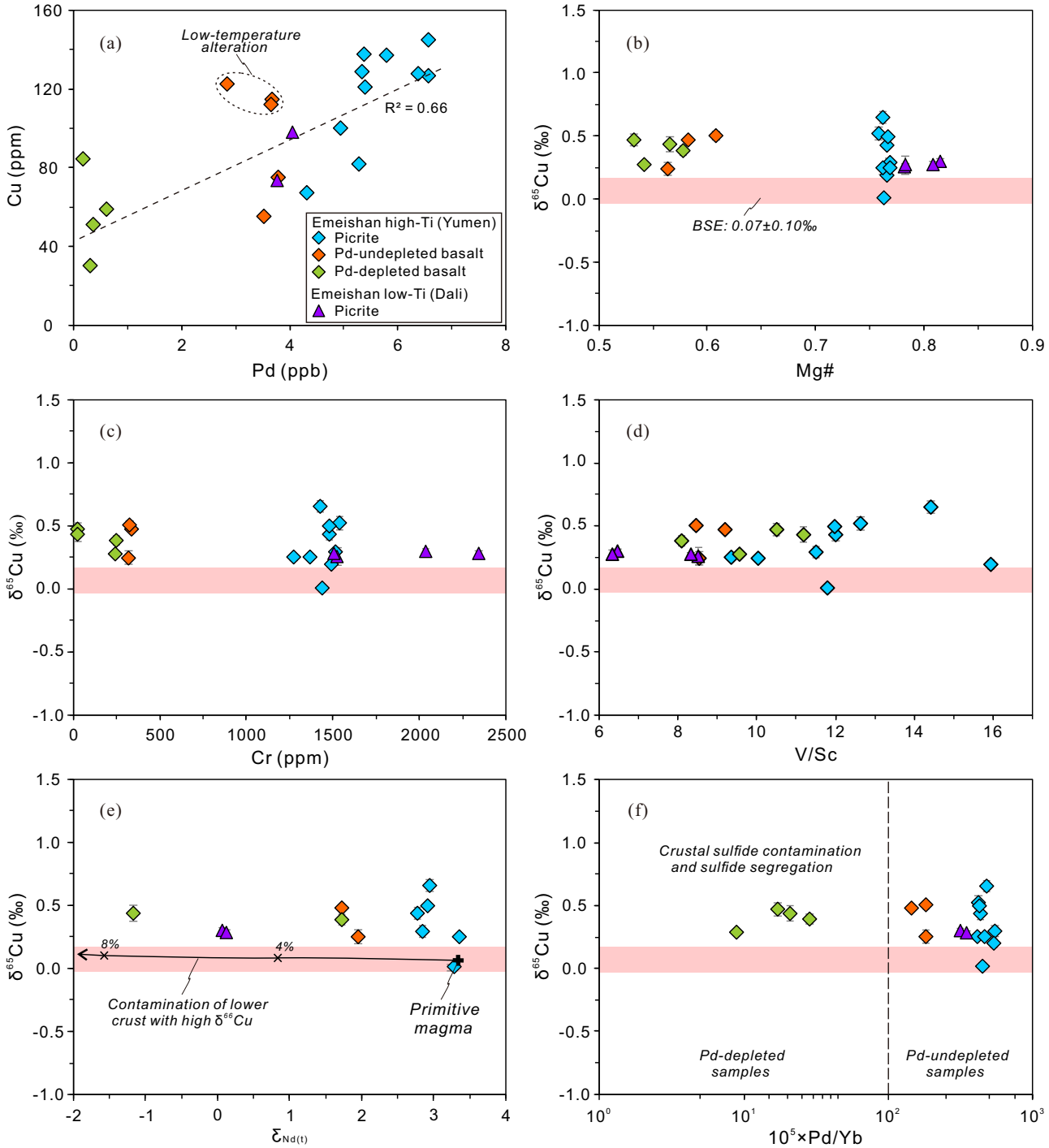

Fig. 3 | Whole-rock δ^{65}Cu and Cu content correlations with geochemical proxies constraining magmatic processes in the Emeishan lavas. Whole-rock Cu versus Pd (**a**), and δ^{65}Cu versus Mg# (**b**), Cr (**c**), V/Sc (**d**), $\varepsilon_{Nd(t)}$ (**e**), and $10^5 \times$ Pd/Yb (**f**). Compositions of end-members for binary mixing model are listed in Supplementary Data 2. Error bars are 2 SD.

+0.16‰)[16,23]. In contrast, other studies attribute δ^{65}Cu variations in massif peridotites and magmatic Ni-Cu deposits to sulfide segregation processes[40,46,56]. While future research is needed to reconcile discrepancies in Cu isotope behavior between sulfide and silicate melt, the lack of systematic δ^{65}Cu variations among Emeishan high-Ti samples (including Yumen picrites, Pd-depleted basalts, and Pd-undepleted basalts) suggests that sulfide segregation in our Pd-depleted basalt samples did not induce substantial Cu isotope fractionation.

Studies of non-metasomatized mantle peridotites and mantle-derived volcanic rocks with varying degrees of melting (e.g., MORB, OIB, and komatiite) show these rocks have similar Cu isotope compositions, leading some researchers to suggest that Cu isotope fractionation during mantle melting is minimal[16,23]. However, the negative correlation observed between δ^{65}Cu values and Al_2O_3 contents of mantle peridotites, though subtle, suggests that lighter ^{63}Cu preferentially enters the melt during partial melting of mantle rocks[56]. This observation appears at odds with the relatively high δ^{65}Cu values (from 0.20‰ to 0.65‰) measured in most Emeishan picrites and basalts, except for one picrite (δ^{65}Cu = 0.01 ± 0.03‰, 2σ) and two outliers likely affected by hydrothermal alteration. Moreover, the ELIP mantle source is believed to lack residual sulfide due to a

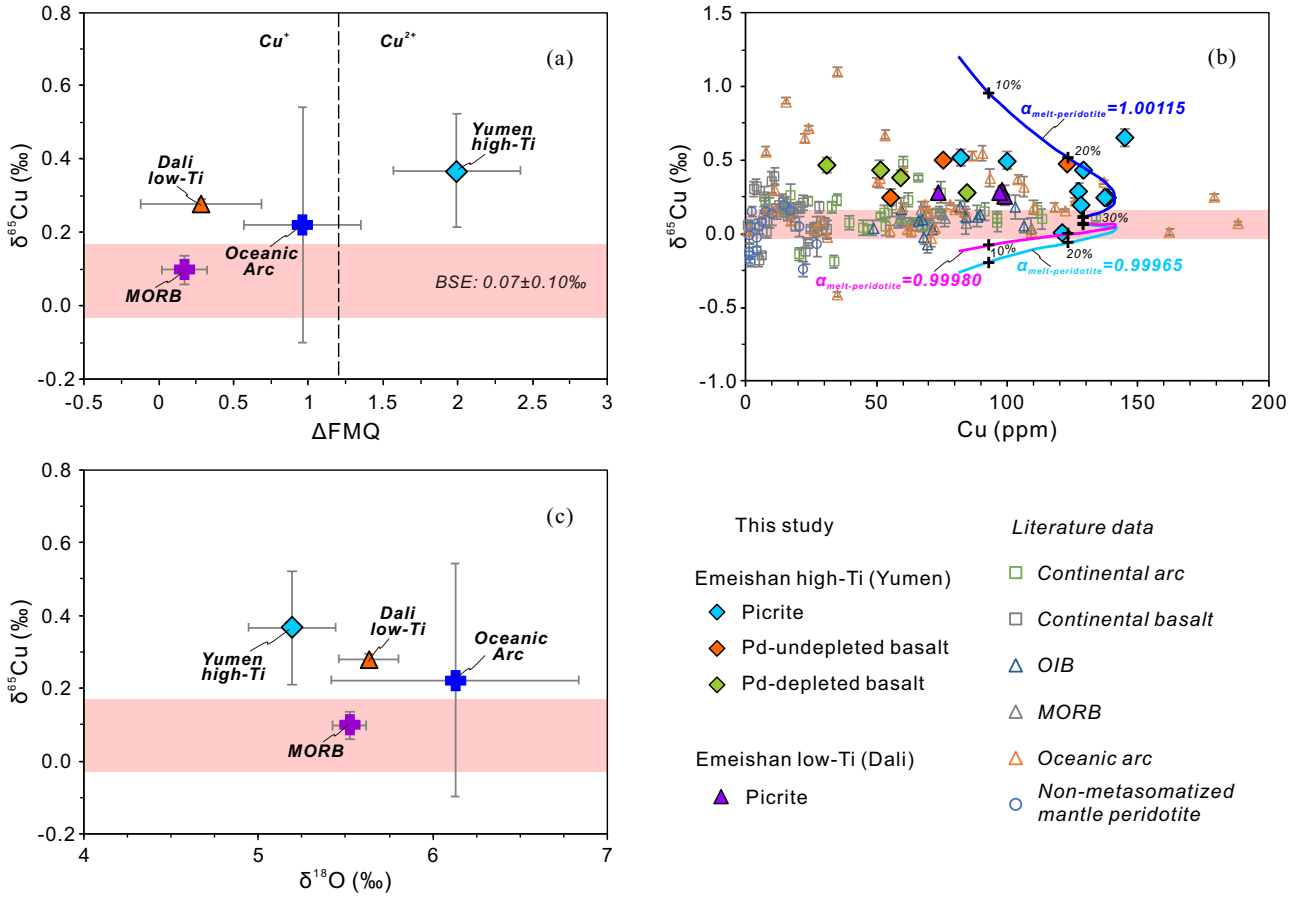

Fig. 4 | Correlations of whole-rock δ^{65}Cu values with geochemical tracers used to infer the mantle source characteristics of the Emeishan lavas. Whole-rock δ^{65}Cu versus ΔFMQ (estimated oxygen fugacity) (**a**), Cu (**b**), and olivine/zircon δ^{18}O (**c**). In Fig. 4a, the dividing line between Cu^{+} and Cu^{2+} is ΔFMQ + 1.2[39]. **b** the modeling curves (solid colored lines) illustrate Cu isotope fractionation during mantle partial melting by Rayleigh fractionation model at variable Cu isotope fractionation factors ($\alpha_{melt\text{-}peridotite}$) (see text and Supplementary Note 2 for details). Cu isotope sources of literature data are listed in Supplementary Note 2. Data source of oxidation states: the Dali low-Ti and Yumen high-Ti magmas[30]; MORB and Oceanic Arc[71]. Data source of oxygen isotopes: the Dali low-Ti and Yumen high-Ti magmas[22,28]; mantle value[72] and oceanic arc[73]. Error bars for δ^{65}Cu are 2 SD. Error bars of average ΔFMQ and δ^{18}O values are 1 standard deviation.

high degree of melting and/or elevated oxygen fugacity, leading to sulfide undersaturation in the silicate melts[29]. This interpretation is supported by the high Pd contents measured in the Emeishan picrites and basalts[44,47]. Consequently, we propose that during partial melting, sulfides in the mantle source were fully melted and depleted, releasing their Cu into the silicate melt. Despite ongoing debates regarding the extent of Cu isotope fractionation among different mineral phases, this process does not appear to induce substantial Cu isotope fractionation in Emeishan magmas.

In summary, despite undergoing complex petrogenetic processes (including fractional crystallization, crustal contamination, and sulfide melt segregation), the elevated δ^{65}Cu signatures of the Emeishan lavas largely reflect the compositional characteristics of their mantle source. These signatures were not substantially modified by subsequent magmatic evolution.

The origin of heavy Cu isotope composition

Four potential mechanisms have been proposed to account for the heavy Cu isotope composition in the mantle source, including (1) the partial melting of mantle under oxidizing conditions[17]; (2) the mantle melting and melt migration-reaction[56]; (3) the involvement of metasomatized subcontinental lithospheric mantle (SCLM)[18]; and (4) the addition of subducted components with high δ^{65}Cu values[23].

First, experimental studies have shown that copper speciation in silicate melt is redox-dependent: Cu^{+} dominates under relatively reduced conditions (ΔFMQ ≤ +1.2), while Cu^{2+} prevails under oxidizing conditions (ΔFMQ ≥ +1.2)[39]. This redox control may influence Cu isotope fractionation, as Cu^{2+} preferentially incorporates isotopically heavier ^{65}Cu over lighter ^{63}Cu, leading to ^{65}Cu enrichment in oxidized silicate melts during mantle melting[41]. Empirical support for this mechanism comes from studies of magmatic Ni–Cu deposits, where positive correlations between the δ^{65}Cu values of chalcopyrite separates and magma fO_2 values have been reported[13]. In ELIP, previous studies[29,30] suggested that the fO_2 values of Emeishan high-Ti magmas range from FMQ + 1.1 to FMQ + 2.6, which are higher than those of the Emeishan low-Ti magmas (ranging from FMQ − 0.5 to FMQ + 0.5). However, both high-Ti and low-Ti lavas in the ELIP exhibit heavy Cu isotope compositions (Fig. 4a), suggesting that the mantle melting under oxidizing conditions cannot explain the elevated δ^{65}Cu values in Emeishan picrites and basalts.

To quantitatively assess Cu behavior during mantle melting, we modeled Cu concentrations in primitive melts at varying degrees of melting using the approach of Lee et al.[49] and calculated their δ^{65}Cu values using a simple Rayleigh distillation model with different Cu isotope fractionation factors ($\alpha_{melt\text{-}peridotite}$) between mantle-derived melts and residual peridotite. This model assumes an initial mantle Cu concentration of 40 ppm with a δ^{65}Cu value of 0.07 ± 0.10‰, and a Cu partition coefficient between sulfide and melt ($D^{Cu}_{sulfide/melt}$) of 800[49]. Under these assumptions, Cu behaves as a compatible element before sulfide exhaustion, remaining largely retained in the residual mantle. However, once sulfides are fully depleted at >20% partial melting[49], Cu transitions to an incompatible element, leading to a shift in its partitioning behavior. This results in a distinct inflection point in Cu behavior at ~25% melting (Fig. 4b), which is consistent with estimates that Emeishan picrites formed through 16% to 30% partial melting of a

plume-head[57,58]. By adjusting the fractionation coefficients ($\alpha_{melt\text{-}peridotite}$), we successfully reproduced the highest $\delta^{65}Cu$ value observed in the Emeishan picrites at ~20% partial melting using an $\alpha_{melt\text{-}peridotite}$ of 1.00015 (Fig. 4b).

If such a high $\alpha_{melt\text{-}peridotite}$ value is common under oxidizing conditions, it could imply that the heavy Cu isotope compositions may be prevalent in global arc basalts, particularly given that many arc magmas exhibit fO_2 values exceeding ΔFMQ + 1. This interpretation is consistent with observations from the Mariana Arc, where basaltic lavas display higher $\delta^{65}Cu$ values (between +0.38 and +0.67‰) than mantle value[17]. However, mantle-like $\delta^{65}Cu$ values have been reported in Izu-Bonin-Mariana arc-related volcanic rocks even though these systems also record high fO_2 values (ΔFMQ > +1)[24]. These contrasting observations suggest that redox-controlled Cu isotope fractionation may not systematically occur during mantle melting. Instead, additional factors may contribute to the high $\delta^{65}Cu$ value observed in basaltic lavas from the Mariana Arc. For example, sulfide undersaturation during melting could retain all Cu in the melt phase, rendering its Cu isotope composition insensitive to oxygen fugacity. Alternatively, the involvement of serpentinite-derived sulfate-rich fluids, which may carry high $\delta^{65}Cu$ values, could modify the Cu isotope compositions of sub-arc mantle sources[17].

Second, the elevated $\delta^{65}Cu$ values (up to 0.38‰) observed in massif peridotites from Ivrea-Verbano Zone (Italian Alps) have been attributed to the removal of sulfides enriched in lighter ^{63}Cu during partial melting, leaving residual mantle peridotites enriched in heavier ^{65}Cu isotopes[56]. However, the Emeishan high-Ti lavas were interpreted as decompression melting of a deep-seated mantle plume of peridotitic composition originating from Earth's deep interior (e.g., the lower mantle)[28]. Unlike metasomatized SCLM, this ELIP plume source remains largely unaffected by subduction-related processes (e.g., metasomatism from slab-derived fluids/melts) or melt–rock interaction processes associated with upper mantle magmatism. Moreover, several Emeishan high-Ti lavas have much higher $\delta^{65}Cu$ values than 0.38‰. Thus, while sulfide extraction during melting drives Cu isotope fractionation in the Ivrea-Verbano system, the Emeishan lavas derive from a mantle source isolated from subduction zones and shallow mantle processes, likely preserving Cu isotope signatures of primitive magmas.

Third, some rocks derived from metasomatized SCLM can exhibit high $\delta^{65}Cu$ values[18]. This enrichment may arise from serpentinite-derived, sulfate-rich fluids, which are known to enrich the mantle wedge with heavier ^{65}Cu through redox-driven processes, as sulfate (SO_4^{2-}) facilitates the preferential incorporation of isotopically heavier ^{65}Cu into mantle rocks[17]. The Yangtze craton, which underwent multiple subduction events (such as the Neoproterozoic Panxi subduction zone)[59], may host a metasomatized lithospheric mantle with elevated $\delta^{65}Cu$ values due to prolonged interaction with such fluids. If the Emeishan mantle plume interacted with this metasomatized SCLM during ascent, it could theoretically generate melts with high $\delta^{65}Cu$ values. However, two lines of evidence argue against this hypothesis. First, previous studies[22] have proposed that the Emeishan low-Ti basalts originated from metasomatized lithospheric mantle, whereas the Emeishan high-Ti basalts were derived from the deep mantle plume itself. While the Emeishan low-Ti picrites might have originated from a metasomatized SCLM, as inferred from elevated $\delta^{18}O$ values (5.3–6.0‰) in primitive olivine phenocrysts[22], the Dali low-Ti picrites, which also exhibit high $\delta^{18}O$ values, have slightly lower $\delta^{65}Cu$ values than those of the Emeishan high-Ti picrites. This inconsistency challenges the hypothesis that an important contribution from a metasomatized lithospheric mantle with high $\delta^{65}Cu$ values is responsible for the heavy Cu isotope composition observed in Emeishan lavas (Fig. 4c). Second, the $\delta^{65}Cu$ values of the Emeishan samples show no clear correlations with geochemical indicators for slab-derived fluid/melt contributions (e.g., Ba/La, Ce/Pb, Ba/Th, and Th/Yb; Fig. S3), inconsistent with the involvement of metasomatized SCLM. Thus, while minor contamination by metasomatized SCLM cannot be entirely excluded, its contribution to the high $\delta^{65}Cu$ values in Emeishan lavas is likely small.

Finally, recent studies[18,28,31,44,48] support the hypothesis that ELIP likely originated from a mantle source of peridotitic composition. However, geochemical evidence from primitive magma compositions inferred from melt inclusions, trace element systematics, and oxygen isotope compositions of olivine phenocrysts suggests minor contributions from recycled subducted components in the mantle source[22,28,60]. While oxidizing conditions may enhance the enrichment of heavier Cu isotope (^{65}Cu) in melts, the addition of recycled components with heavy-Cu isotope signature is most likely the main factor in raising the $\delta^{65}Cu$ values of the Emeishan lavas. Therefore, our results highlight recycled subducted components as a key mechanism for generating heterogeneous Cu isotope compositions in the deep mantle. This process likely dominates over redox-driven Cu isotope fractionation effects, particularly in systems where ancient slab-derived materials contribute to mantle source heterogeneity.

Implication for deep copper-rich sulfide cycle

This study reports substantial heavy Cu isotope enrichment (elevated $\delta^{65}Cu$ value) in intraplate basalts sourced from the deep mantle. The high $\delta^{65}Cu$ values observed in Emeishan picrites and basalts suggest the incorporation of recycled components with $\delta^{65}Cu$ values in the mantle source. These findings have critical implications for understanding the cycling of Cu-rich sulfides in deep mantle.

Cu isotopes have been well-documented to undergo substantial fractionation during low- to medium-temperature geological processes, including chemical weathering[36], Cu deposition in hydrothermal environments (e.g., porphyry and skarn deposits)[61,62], sedimentary processes[63], and the formation of Cu-bearing sulfides in black smokers[64]. For example, in the Emeishan Pd-undepleted basalts (Yumen), three outliers (two of which have extreme $\delta^{65}Cu$ values) are attributed to alteration by low-temperature fluids. In contrast, under high-temperature magmatic conditions, processes such as progressive sulfide segregation or melt-peridotite reactions, while theoretically capable of inducing Cu isotope fractionation in the lithospheric mantle[51,56], do not appear to drive substantial isotopic variability. Both our data and previous studies confirm smaller Cu isotope variation during the magmatic evolution of basaltic melts (including fractional crystallization or melt migration) than observed in most Emeishan basalts and picrites.

Oceanic igneous rocks (e.g., OIBs and MORBs) typically exhibit mantle-like Cu isotope compositions, whereas continental intraplate basalts display a wider range of $\delta^{65}Cu$ values, reflecting their complex petrogenic processes (Fig. 1). During the subduction of oceanic igneous rocks, several observations indicate that subduction metamorphism has a limited impact on the Cu isotope signatures of subducting slabs. For example, Busigny et al.[65] suggested that Cu loss from metagabbro to subduction fluids is minimal during subduction metamorphism, based on Cu-N isotope systematics in Alpine meta-gabbros; Cu depletion instead occurs mainly during hydrothermal alteration on the seafloor. Similarly, Liu et al.[46] found no systematic variation between Cu and $\delta^{65}Cu$ values in a suite of subduction-related prograde metamorphic rocks (from greenschist to eclogite facies), further supporting limited Cu mobility during slab dehydration. In addition, most modern volcanic rocks from island arcs have mantle-like $\delta^{65}Cu$ values despite varying trace element ratios (e.g., Ba/Nb and Th/Yb)[23,24,46,53]. These observations collectively imply that subducted materials appear capable of preserving their original Cu isotope compositions through the subduction cycle, enabling recycled components to retain surficial Cu isotope signatures in the deep mantle.

As shown in Fig. 1, Fe-Mn crusts[66] and black smokers[64], formed in Earth's surface systems and enriched in sulfide minerals, exhibit remarkably higher $\delta^{65}Cu$ values. Fe-Mn crusts are characterized by elevated $\delta^{65}Cu$ and $\delta^{66}Zn$ values along with high Mn concentrations[66]; these signatures could theoretically contribute to mantle sources after being subducted. However, primitive magmas of the ELIP exhibit Zn isotope compositions akin to those of MORB ($\delta^{66}Zn$: ~0.3‰)[67] and do not show Mn enrichment[60], ruling out the assimilation of subducted Fe-Mn crust as a dominant mechanism. Instead, we propose that subducted, ^{65}Cu-enriched crustal sulfides (e.g., black smokers) represent the more plausible source component, considering

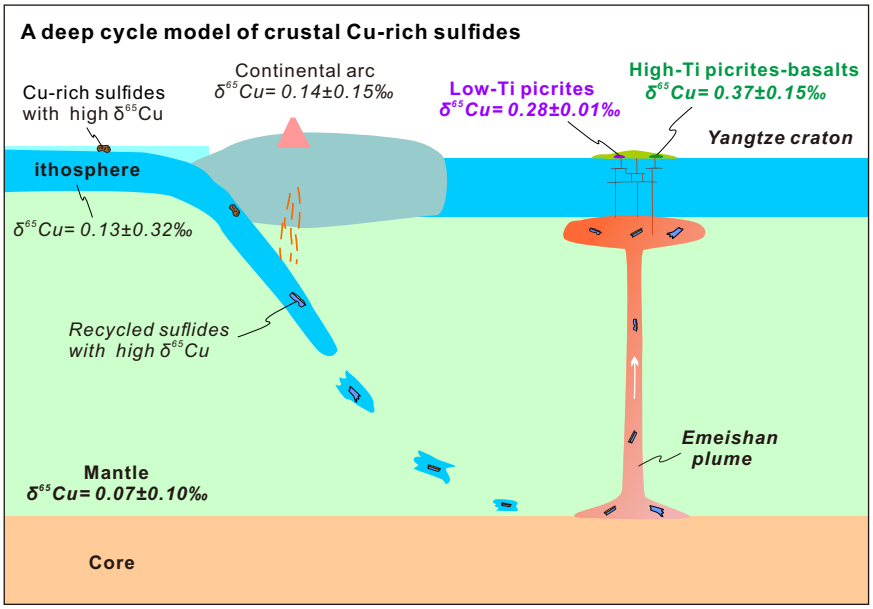

Fig. 5 | Schematic model showing a deep cycle of crustal Cu-rich sulfides tracked by the heavy Cu isotope composition from the ELIP picrites-basalts. Cu isotope data source of different geological reservoirs is listed in Supplementary Note 2. See texts for further explanations. Error bars are 2 SD.

that Cu is predominantly hosted in sulfides in both Earth's surface systems and deep-seated systems.

Our findings, along with previous studies on the ELIP, support a multi-stage deep-cycle model for Cu-rich sulfides (Fig. 5). The cycle begins with the subduction of Cu-rich materials having high δ^{65}Cu values (e.g., active black smokers formed in a submarine hydrothermal system) into the deep mantle. As the chemically heterogeneous Emeishan mantle plume ascends, partial melting of mantle components containing these subducted materials with high δ^{65}Cu values generates high-Ti and low-Ti magmas. A minor contribution from subducting oceanic crust may explain the elevated Fe and Ti abundances in high-Ti melts and olivines with slightly higher δ^{18}O values than mantle values from low-Ti melts. The incorporation of subducted crustal sulfides with high δ^{65}Cu values contributes to the heavy Cu isotope compositions observed in the Emeishan lavas. The incorporation of variable proportions of these recycled components could account for the distinct δ^{65}Cu observed between high-Ti and low-Ti picrites and basalts within the ELIP. Finally, magmatic processes, including fractional crystallization, sulfide melt segregation, and crustal contamination, produce the diverse geochemical signatures observed in the Emeishan picrites and basalts[26,44,48,58].

This multi-stage deep-cycle model provides a simplified explanation based on interpretations of currently available data. While we suggest the involvement of material geochemically akin to black-smoker sulfides that represents the most plausible known Cu reservoir with the requisite heavy isotope signature, the precise mechanism and quantity of its incorporation into the mantle source of Emeishan picrite-basalt suite remain unresolved. Other, as yet unidentified surficial or mantle reservoirs, could potentially bear similar geochemical signatures. However, until such reservoirs are identified, recycled crustal sulfides within a deep mantle plume source remain the most plausible and preferred explanation for the Cu-rich materials with high δ^{65}Cu values observed in the Emeishan samples. More complex models involving multiple processes and components cannot be ruled out. For example, metasomatisms of the SCLM by melts from a plume containing recycled sulfides, followed by later plume ascent incorporating this modified signature. Nevertheless, the fundamental origin of the high-δ^{65}Cu signature is most likely explained by recycled crustal sulfides within the deep mantle plume source.

In conclusion, this study demonstrates that Cu isotope compositions (δ^{65}Cu) serve as an effective tracer for identifying recycled, Cu-rich crustal components within the deep mantle. The heavy Cu isotope signatures observed in the Emeishan picrite-basalt suite provide strong evidence for subduction-driven recycling of crustal sulfides (possibly incorporating minor metasomatic SCLM) into mantle-derived magmas. Further investigation into deep mantle copper reservoirs is crucial for elucidating the mechanisms and pathways of the deep Cu-S cycle, as well as for understanding the long-term cycling of crustal sulfides within Earth's interior. Such insights will substantially enhance our understanding of material exchange between the crust and mantle and contribute to a more comprehensive view of Earth's geochemical evolution over geological timescales.

Methods

Whole-rock major-trace element analyses

Loss on ignition (LOI) was measured by recording the weight loss of sample powder after heating at ~1000 °C for ~1.5 hours. For major element analysis, ~0.6 g of the dried sample was mixed with ~6 g of lithium tetraborate and fused at ~1050 °C to form a glass disk, which was then analyzed using X-ray fluorescence spectrometry at the Rock–Mineral Preparation and Analysis Lab, Institute of Geology and Geophysics, Chinese Academy of Sciences (IGGCAS). The analytical precision for major elements is better than 5%.

Whole-rock trace element concentrations were determined using an Agilent 7500a inductively-coupled-plasma mass-spectrometer at IGGCAS, with detailed analytical procedures described in a previous study[31]. The analytical precisions for most trace elements are generally better than 10%.

Cu isotope composition analysis

Sample digestion and column chemistry for whole-rock Cu isotope analyses were carried out at the School of Earth System Science (SESS), Tianjin University, following a modified procedure outlined in previous studies[68,69]. About 20–50 mg of sample powders were weighted into Teflon beakers based on their Cu concentrations to obtain ~1.2 mg of Cu. Samples were dissolved in a mixture of HNO_3-HF-HCl at ~120 °C for ~72 hours. After complete dissolution, the samples were dried, with HF removed by adding and evaporating concentrated HNO_3. Subsequently, about 1 mL of 8.2 M HCl + 0.03% H_2O_2 were added to the beaker and evaporated to dryness at ~95 °C. This process was repeated three times. The final material was dissolved in ~1 mL of 8.2 M HCl + 0.03% H_2O_2 for ion-exchange separation. The sample solution was loaded on ~1 mL of pre-cleaned AG MP-1 M resin (Bio-Rad, 100–200 mesh), with matrix elements eluted using ~4 mL of 8.2 M HCl + 0.03% H_2O_2 solution, while Cu was collected in ~11 mL of the same solution. The column separation procedure was repeated to ensure Cu purity. The Cu fractions were dried, converted to nitrate form, and re-dissolved in 2% HNO_3 for Cu isotope ratio analysis. The Cu recovery yields were 99 ± 1% (1 SD, n = 19), with total procedural blank typically <1 ng.

Copper isotope ratios in an ~200 ng/g Cu solution were measured using a Neptune Plus MC-ICP-MS at SESS, Tianjin University. A sample-

standard bracketing method was employed to correct for instrumental mass bias and drifts during measurement. Cu concentrations in the samples were verified and adjusted to match the Cu standard solution within 10%. Each analysis consisted of one block of 90 cycles, with each cycle lasting ~2 seconds. Cu isotope ratios are reported in delta notation relative to the standard reference material (SRM) NIST 976 (expressed as follows: $\delta^{65}Cu = [(^{65}Cu/^{63}Cu)_{sample}/(^{65}Cu/^{63}Cu)_{NIST\ 976} - 1] \times 1000‰$). Analysis of the BHVO-2 standard processed in the same way as unknown samples, yielded a $\delta^{65}Cu$ value of 0.15 ± 0.03‰ (2 SD, $n = 5$), which is consistent with previously reported values[17,23].

Data availability

All data needed to evaluate the conclusions in the paper are present in the paper and/or the Supplementary Information and Supplementary Data.

Received: 21 November 2024; Accepted: 10 June 2025;
Published online: 21 June 2025

References

1. Blichert-Toft, J., Albarede, F. & Kornprobst, J. Lu-Hf isotope systematics of garnet pyroxenites from Beni Bousera, Morocco: Implications for basalt origin. *Science* **283**, 1303–1306 (1999).
2. Dixon, J. E., Leist, L., Langmuir, C. & Schilling, J.-G. Recycled dehydrated lithosphere observed in plume-influenced mid-ocean-ridge basalt. *Nature* **420**, 385–389 (2002).
3. Liu, J. et al. Melting of recycled ancient crust responsible for the Gutenberg discontinuity. *Nat. Commun.* **11**, 172 (2020).
4. Hart, S., Hauri, E., Oschmann, L. & Whitehead, J. Mantle plumes and entrainment: isotopic evidence. *Science* **256**, 517–520 (1992).
5. Nielsen, S. G. & Marschall, H. R. Geochemical evidence for mélange melting in global arcs. *Sci. Adv.* **3**, e1602402 (2017).
6. Timmerman, S. et al. Primordial and recycled helium isotope signatures in the mantle transition zone. *Science* **365**, 692–694 (2019).
7. Abouchami, W. et al. Lead isotopes reveal bilateral asymmetry and vertical continuity in the Hawaiian mantle plume. *Nature* **434**, 851–856 (2005).
8. Bennett, V., Esat, T. & Norman, M. Two mantle-plume components in Hawaiian picrites inferred from correlated Os–Pb isotopes. *Nature* **381**, 221–224 (1996).
9. Hofmann, A. W. Mantle geochemistry: the message from oceanic volcanism. *Nature* **385**, 219–229 (1997).
10. Li, S.-G. et al. Deep carbon cycles constrained by a large-scale mantle Mg isotope anomaly in eastern China. *Natl. Sci. Rev.* **4**, 111–120 (2017).
11. Teng, F.-Z., Dauphas, N. & Watkins, J. M. Non-traditional stable isotopes: retrospective and prospective. *Rev. Mineral. Geochem.* **82**, 1–26 (2017).
12. Xue, Q. et al. Tracing black shales in the source of a porphyry Mo deposit using molybdenum isotopes. *Geology* **51**, 688–692 (2023).
13. Zhao, Y. et al. Copper isotope fractionation in magmatic Ni–Cu mineralization systems associated with the variation of oxygen fugacity in silicate magmas. *Geochim. Cosmochim. Acta* **338**, 250–263 (2022).
14. Mathur, R. & Fantle, M. S. Copper isotopic perspectives on supergene processes: Implications for the global Cu cycle. *Elements* **11**, 323–329 (2015).
15. Moynier, F., Vance, D., Fujii, T. & Savage, P. The isotope geochemistry of zinc and copper. *Rev. Mineral. Geochem.* **82**, 543–600 (2017).
16. Savage, P. S. et al. Copper isotope evidence for large-scale sulphide fractionation during Earth's differentiation. *Geochem. Perspect. Lett.* (2015).
17. Chen, Z. et al. Heavy copper isotopes in arc-related lavas from cold subduction zones uncover a sub-arc mantle metasomatized by serpentinite-derived sulfate-rich fluids. *J. Geophys. Res.: Solid Earth* **127**, e2022JB024910 (2022).
18. Kempton, P. D. et al. Cu-isotope evidence for subduction modification of lithospheric mantle. *Geochem. Geophys. Geosyst.* **23**, e2022GC010436 (2022).
19. Blichert-Toft, J., Frey, F. & Albarede, F. Hf isotope evidence for pelagic sediments in the source of Hawaiian basalts. *Science* **285**, 879–882 (1999).
20. Saal, A., Hart, S., Shimizu, N., Hauri, E. & Layne, G. Pb isotopic variability in melt inclusions from oceanic island basalts, Polynesia. *Science* **282**, 1481–1484 (1998).
21. Weis, D. et al. Earth's mantle composition revealed by mantle plumes. *Nat. Rev. Earth Environ.* **4**, 604–625 (2023).
22. Yu, S.-Y. et al. An integrated chemical and oxygen isotopic study of primitive olivine grains in picrites from the Emeishan Large Igneous Province, SW China: Evidence for oxygen isotope heterogeneity in mantle sources. *Geochim. Cosmochim. Acta* **215**, 263–276 (2017).
23. Liu, S.-A. et al. Copper isotopic composition of the silicate Earth. *Earth Planet. Sci. Lett.* **427**, 95–103 (2015).
24. Wang, Z. et al. Copper recycling and redox evolution through progressive stages of oceanic subduction: Insights from the Izu-Bonin-Mariana forearc. *Earth Planet. Sci. Lett.* **574**, 117178 (2021).
25. Chung, S.-L. & Jahn, B-m. Plume-lithosphere interaction in generation of the Emeishan flood basalts at the Permian-Triassic boundary. *Geology* **23**, 889–892 (1995).
26. Xu, Y., Chung, S.-L., Jahn, B-m. & Wu, G. Petrologic and geochemical constraints on the petrogenesis of Permian–Triassic Emeishan flood basalts in southwestern China. *Lithos* **58**, 145–168 (2001).
27. Xiao, L. et al. Distinct mantle sources of low-Ti and high-Ti basalts from the western Emeishan large igneous province, SW China: implications for plume–lithosphere interaction. *Earth Planet. Sci. Lett.* **228**, 525–546 (2004).
28. Yao, J.-H. et al. Olivine O isotope and trace element constraints on source variation of picrites in the Emeishan flood basalt province, SW China. *Lithos* **338**, 87–98 (2019).
29. Bai, Z.-J., Zhong, H., Hu, R.-Z., Zhu, W.-G. & Hu, W.-J. Composition of the chilled marginal rocks of the Panzhihua layered intrusion, Emeishan Large Igneous Province, SW China: Implications for parental magma compositions, sulfide saturation history and Fe–Ti oxide mineralization. *J. Petrol.* **60**, 619–648 (2019).
30. Cao, Y. & Wang, C. Y. Contrasting oxidation states of low-Ti and high-Ti magmas control Ni-Cu sulfide and Fe-Ti oxide mineralization in Emeishan Large Igneous Province. *Geosci. Front.* **13**, 101434 (2022).
31. Wu, Y.-D. et al. Redox heterogeneity of picritic lavas with respect to their mantle sources in the Emeishan large igneous province. *Geochim. Cosmochim. Acta* **320**, 161–178 (2022).
32. Fleet, M., Crocket, J. & Stone, W. Partitioning of platinum-group elements (Os, Ir, Ru, Pt, Pd) and gold between sulfide liquid and basalt melt. *Geochim. Cosmochim. Acta* **60**, 2397–2412 (1996).
33. Li, C., Ripley, E. M., Tao, Y. & Hu, R. The significance of PGE variations with Sr–Nd isotopes and lithophile elements in the Emeishan flood basalt province from SW China to northern Vietnam. *Lithos* **248**, 1–11 (2016).
34. Fernandez, A. & Borrok, D. M. Fractionation of Cu, Fe, and Zn isotopes during the oxidative weathering of sulfide-rich rocks. *Chem. Geol.* **264**, 1–12 (2009).
35. Fujii, T., Moynier, F., Abe, M., Nemoto, K. & Albarède, F. Copper isotope fractionation between aqueous compounds relevant to low temperature geochemistry and biology. *Geochim. Cosmochim. Acta* **110**, 29–44 (2013).
36. Mathur, R. et al. Cu isotopes and concentrations during weathering of black shale of the Marcellus Formation, Huntingdon County, Pennsylvania (USA). *Chem. Geol.* **304**, 175–184 (2012).
37. Guo, Z. et al. Copper isotopic fractionation during seafloor alteration: Insights from altered basalts in the Mariana and Yap Trenches. *J. Geophys. Res. Solid Earth* **127**, e2021JB023597 (2022).

38. Liu, S.-A., Liu, P.-P., Lv, Y., Wang, Z.-Z. & Dai, J.-G. Cu and Zn isotope fractionation during oceanic alteration: Implications for Oceanic Cu and Zn cycles. *Geochim. Cosmochim. Acta* **257**, 191–205 (2019).
39. Liu, X. et al. Partitioning of copper between olivine, orthopyroxene, clinopyroxene, spinel, garnet and silicate melts at upper mantle conditions. *Geochim. Cosmochim. Acta* **125**, 1–22 (2014).
40. Zhao, Y. et al. Copper isotope fractionation during sulfide-magma differentiation in the Tulaergen magmatic Ni–Cu deposit, NW China. *Lithos* **286**, 206–215 (2017).
41. Ehrlich, S. et al. Experimental study of the copper isotope fractionation between aqueous Cu (II) and covellite, CuS. *Chem. Geol.* **209**, 259–269 (2004).
42. Savage, P. S., Moynier, F., Harvey, J. & Burton, K. W. In *AGU Fall Meeting Abstracts*. V53B–V53137.
43. Huang, J., Liu, S.-A., Wörner, G., Yu, H. & Xiao, Y. Copper isotope behavior during extreme magma differentiation and degassing: a case study on Laacher See phonolite tephra (East Eifel, Germany). *Contrib. Mineral. Petrol.* **171**, 1–16 (2016).
44. Yao, J.-H., Zhu, W.-G., Wang, Y.-J., Zhong, H. & Bai, Z.-J. Geochemistry of the Yumen picrites-basalts from the Emeishan large igneous province: implications for their mantle source, PGE behaviors, and petrogenesis. *Lithos* **400**, 106364 (2021).
45. Li, W., Jackson, S. E., Pearson, N. J., Alard, O. & Chappell, B. W. The Cu isotopic signature of granites from the Lachlan Fold Belt, SE Australia. *Chem. Geol.* **258**, 38–49 (2009).
46. Liu, S.-A. et al. Copper isotope evidence for sulfide fractionation and lower crustal foundering in making continental crust. *Sci. Adv.* **9**, eadg6995 (2023).
47. Li, C., Tao, Y., Qi, L. & Ripley, E. M. Controls on PGE fractionation in the Emeishan picrites and basalts: constraints from integrated lithophile–siderophile elements and Sr–Nd isotopes. *Geochim. Cosmochim. Acta* **90**, 12–32 (2012).
48. Xu, R., Liu, Y. & Lambart, S. Melting of a hydrous peridotite mantle source under the Emeishan large igneous province. *Earth Sci. Rev.* **207**, 103253 (2020).
49. Lee, C.-T. A. et al. Copper systematics in arc magmas and implications for crust-mantle differentiation. *Science* **336**, 64–68 (2012).
50. Xia, Y., Kiseeva, E. S., Wade, J. & Huang, F. The effect of core segregation on the Cu and Zn isotope composition of the silicate Moon. https://www.geochemicalperspectivesletters.org/article1928/# (2019).
51. Zou, Z. et al. Copper isotope variations during magmatic migration in the mantle: Insights from mantle pyroxenites in Balmuccia peridotite massif. *J. Geophys. Res. Solid Earth* **124**, 11130–11149 (2019).
52. Tang, D. et al. Sulfur and copper isotopic signatures of chalcopyrite at Kalatongke and Baishiquan: Insights into the origin of magmatic Ni-Cu sulfide deposits. *Geochim. Cosmochim. Acta* **275**, 209–228 (2020).
53. Wang, Z. et al. Evolution of copper isotopes in arc systems: Insights from lavas and molten sulfur in Niuatahi volcano, Tonga rear arc. *Geochim. Cosmochim. Acta* **250**, 18–33 (2019).
54. Patten, C., Barnes, S.-J., Mathez, E. A. & Jenner, F. E. Partition coefficients of chalcophile elements between sulfide and silicate melts and the early crystallization history of sulfide liquid: LA-ICP-MS analysis of MORB sulfide droplets. *Chem. Geol.* **358**, 170–188 (2013).
55. Peters, B. J., Shahar, A., Carlson, R. W., Day, J. M. & Mock, T. D. A sulfide perspective on iron isotope fractionation during ocean island basalt petrogenesis. *Geochim. Cosmochim. Acta* **245**, 59–78 (2019).
56. Huang, J., Huang, F., Wang, Z., Zhang, X. & Yu, H. Copper isotope fractionation during partial melting and melt percolation in the upper mantle: Evidence from massif peridotites in Ivrea-Verbano Zone, Italian Alps. *Geochim. Cosmochim. Acta* **211**, 48–63 (2017).
57. Yu, S.-Y. et al. Controls of mantle source and condition of melt extraction on generation of the picritic lavas from the Emeishan large igneous province, SW China. *J. Asian Earth Sci.* **203**, 104534 (2020).
58. Zhang, Z., Mahoney, J. J., Mao, J. & Wang, F. Geochemistry of picritic and associated basalt flows of the western Emeishan flood basalt province, China. *J. Petrol.* **47**, 1997–2019 (2006).
59. Yao, J.-H. et al. Petrogenesis and ore genesis of the Lengshuiqing magmatic sulfide deposit in southwest China: Constraints from chalcophile elements (PGE, Se) and Sr-Nd-Os-S isotopes. *Econ. Geol.* **113**, 675–698 (2018).
60. Ren, Z.-Y. et al. Primary magmas and mantle sources of Emeishan basalts constrained from major element, trace element and Pb isotope compositions of olivine-hosted melt inclusions. *Geochim. Cosmochim. Acta* **208**, 63–85 (2017).
61. Li, W., Jackson, S. E., Pearson, N. J. & Graham, S. Copper isotopic zonation in the Northparkes porphyry Cu–Au deposit, SE Australia. *Geochim. Cosmochim. Acta* **74**, 4078–4096 (2010).
62. Maher, K. C. & Larson, P. B. Variation in copper isotope ratios and controls on fractionation in hypogene skarn mineralization at Coroccohuayco and Tintaya, Peru. *Econ. Geol.* **102**, 225–237 (2007).
63. Asael, D., Matthews, A., Bar-Matthews, M. & Halicz, L. Copper isotope fractionation in sedimentary copper mineralization (Timna Valley, Israel). *Chem. Geol.* **243**, 238–254 (2007).
64. Rouxel, O., Fouquet, Y. & Ludden, J. N. Copper isotope systematics of the Lucky Strike, Rainbow, and Logatchev sea-floor hydrothermal fields on the Mid-Atlantic Ridge. *Econ. Geol.* **99**, 585–600 (2004).
65. Busigny, V., Chen, J., Philippot, P., Borensztajn, S. & Moynier, F. Insight into hydrothermal and subduction processes from copper and nitrogen isotopes in oceanic metagabbros. *Earth Planet. Sci. Lett.* **498**, 54–64 (2018).
66. Little, S. H., Vance, D., Walker-Brown, C. & Landing, W. M. The oceanic mass balance of copper and zinc isotopes, investigated by analysis of their inputs, and outputs to ferromanganese oxide sediments. *Geochim. Cosmochim. Acta* **125**, 673–693 (2014).
67. Yang, C. & Liu, S. A. Zinc isotope constraints on recycled oceanic crust in the mantle sources of the Emeishan large igneous province. *J. Geophys. Res. Solid Earth* **124**, 12537–12555 (2019).
68. Hou, Q. et al. Use of Ga for mass bias correction for the accurate determination of copper isotope ratio in the NIST SRM 3114 Cu standard and geological samples by MC-ICPMS. *J. Anal. Spectrom.* **31**, 280–287 (2016).
69. Zhang, T. et al. Copper and Zinc isotope signatures in scleratinian corals: Implications for Cu and Zn cycling in modern and ancient ocean. *Geochim. Cosmochim. Acta* **317**, 395–408 (2022).
70. Fellows, S. A. & Canil, D. Experimental study of the partitioning of Cu during partial melting of Earth's mantle. *Earth Planet. Sci. Lett.* **337**, 133–143 (2012).
71. Cottrell, E. et al. Oxygen fugacity across tectonic settings. In *Magma redox geochemistry*, 33–61 (2021).
72. Mattey, D., Lowry, D. & Macpherson, C. Oxygen isotope composition of mantle peridotite. *Earth Planet. Sci. Lett.* **128**, 231–241 (1994).
73. Yao, J. et al. Variations of Sr–Nd–Hf–O isotopes and redox conditions across a Neoproterozoic arc magmatic belt in the western margin of the Yangtze craton. *Chem. Geol.* **640**, 121735 (2023).

Acknowledgements

This work was financially supported by the National Natural Science Foundation of China (Nos. 42421003, 42206051, 42473007, 41625012). We gratefully acknowledge David Fox and two anonymous reviewers for their constructive comments and suggestions, and Editor Holly Stein and Associate Editor Carolina Ortiz Guerrero for the constructive comments and efficient editorial handling. All these comments significantly improved the manuscript. We thank Yan-Jun Wang and Qingfeng Mei for their help with sample collection, Dr. Chusi Li of Indiana University for useful discussions and suggestions. No sampling permissions were required.

Author contributions

J.H.Y.: conceptualization, visualization, writing-original draft, writing-review & editing. W.Y.: conceptualization, supervision, writing-original draft, writing-review & editing. Z.R.W.: methodology, visualization, writing-review & editing. F.M.: visualization, writing review, and editing. W.G.Z.: investigation, visualization. Y.D.W.: methodology, investigation. Y.C.A.: methodology. J.B.C.: visualization, supervision, writing-review & editing.

Competing interests

The authors declare no competing interests.

Additional information

Supplementary information The online version contains supplementary material available at https://doi.org/10.1038/s43247-025-02468-x.

Correspondence and requests for materials should be addressed to Wei Yuan or Jiubin Chen.

Peer review information *Communications Earth & Environment* thanks David Fox and the other, anonymous, reviewer(s) for their contribution to the peer review of this work. Primary Handling Editors: Holly Stein, Carolina Ortiz Guerrero, and Alireza Bahadori. A peer review file is available.